Whole Body Cooling Hypothermia Treatment Modelling using a Finite Element Thermoregulation Model

Ana Beatriz C. G. Silva

anabeatrizgonzaga@coc.ufrj.br

Federal University of Rio de Janeiro

Ilha do Fundão, CEP 21945-970, Rio de Janeiro, Brazil

Luiz Carlos Wrobel

luiz.wrobel@brunel.ac.uk

Brunel University

Uxbridge UB8 3PH, United Kingdom

Fernando Luiz B. Ribeiro

fernando@coc.ufrj.br

Federal University of Rio de Janeiro

Ilha do Fundão, CEP 21945-970,Rio de Janeiro, Brazil

Abstract. *This paper presents a thermoregulation model using the finite element method to perform numerical analyses of brain cooling procedures as a contribution to the investigation on the use of therapeutic hypothermia after ischemia in adults. The use of computational methods can aid clinicians to observe body temperature using different cooling methods without the need of invasive techniques, and can thus be a valuable tool to assist clinical trials simulating different cooling options that can be used for treatment. In this work, we developed a FEM package applied to the solution of the continuum bioheat Pennes equation. Blood temperature changes were considered using a blood pool approach and a lumped analysis for intravascular catheter method of blood cooling. Some analyses are performed using a three-dimensional mesh based on a complex geometry obtained from computed tomography medical images, considering a cooling blanket and a intravascular catheter. A comparison is made between the results obtained and the effects of each case in brain temperature reduction in a required time is analyzed.*

Keywords: *brain cooling, finite element method, hypothermia treatment, thermoregulation*

1 INTRODUCTION

Therapeutic hypothermia is a medical treatment used to reduce the damages caused by ischemic diseases that lead to a hipoxic condition in the internal organs. The brain is the most vunerable organ to this condition (Tisherman and Sterz, 2005), which can be caused by cardiac arrest, arteries oclusion and cerebral trauma. After an hypoxic-ischemic event, there is a critical time when secondary factors such as hypotension, hypoxia, hyperglycemia and hyperthermia may occur and cause brain cell damage (Hickey and J.Painter, 2006), causing deterioration on brain cells. The hypothermia treatment consists in reducing the brain temperature to a mild ($35 - 36^oC$) or moderate ($32 - 35^oC$) hypothermia state, depending on the type of intervention. This reduction increases neuroprotection and limits the damage in the affected tissues.

In animal trials, an improvement of neurological sequels was observed after hypothermia treatment within six hours of injury (Eicher et al., 2005), even when only a small reduction ($1 - 2^oC$)is achieved (Diao et al., 2003). Nozari et al. (2006) states that mild or moderate hypothermia induced during cardiopulmonary resuscitation opens a window of time to restore spontaneous circulation, minimizes organ injury and enables intact survival in dogs. The study suggests that a mild hypothermia treatment after cardiopulmonary resuscitation during a cardiac arrest enables intact survival if the cooling process begins during the critical window, allowing a considerable time for transportation of cardiac arrest victims patients to a hospital. In Colbourne and Corbett (1994), results of trials for cardiac arrest in gerbils show that 24 hours of post-ischemic hypothermia increases neuroprotection and reduces death.

For adults, the type of hypothermia method used during the treatment is usually whole body cooling (WBC) using thermal blankets and thermal mattress, the application of ice pads or ice packs in different parts of the body, intracarotid infusion of cold fluid or intravascular catheter. The efficacy of each method is still under discussion, as there is no consense so far about which of them would have a better effect in reducing sequels.

The lack of detailed clinical information about the time to reach target temperature, methodology of the procedure and temperature measurements makes it difficult to establish a standard protocol for WBC techniques. Sometimes methods used are not adequately explained. Yang et al. (2006) reduced the brain temperature to 35^oC within one hour and to $32 - 35^oC$ within $3 - 4$ hours. In case of cardiac arrest, the International Liaison Committe on Resuscitation recommends that unconscious adults should be cooled to $32 - 34^oC$ for 12 to 24 hours (Nolan et al., 2003).

A thermoregulation model capable of simulating a real cooling therapy can be used to assist clinical trials for hypothermia techniques, simulating the best options to be used during the research and improving low cost methods that could be used in public hospitals and clinics that can not afford expensive techniques. It can also become an integrated part of commercial cooling systems, improving their efficiency and providing on-time body temperature that can be used to adjust the system to the correct set up during the procedure.

In recent decades, several models were developed to reproduce the human thermoregulatory behavior, from two node models of core and skin heat balances to more complex multi-segment models of the human body and its thermoregulatory responses Fiala et al. (1999). The work of Al-Othmani et al. (2008) uses an arterial system model to calculate blood flow in the core tissue and a bioheat model to determine skin temperature for nude and clothed human body in transient non-uniform environments. The model presented in Fiala (1998) incorporates the

body heat losses considering a non-uniform temperature distribution in the skin, regulatory responses, properties of clothing used and various environmental conditions such as extreme temperatures, wind speed and solar radiation. Xiang and Liu (2008) uses a compartmental model of 12 body segments and a blood compartment to simulate whole body hyperthermia treatments for tumours. In Laszczyk and Nowak (2015b); Silva et al. (2016), a heat transfer model was implemented to simulate hypothermia treatment in neonates using a three-dimensional geometry obtained from magnetic resonance imaging (MRI) scans. In Zhu et al. (2009), a numerical model for whole body intravascular cooling was developed and applied to a human body consisting of a cylinder of one material and a combination of components representing torso, head and limbs. The work calculated a $1.2^oC/hour$ cooling rate for a cooling capacity of $100W$ and suggests the method can be used to reduce critical fever of 40.0^oC or hypothermia of 34.0^oC in less than 3 hours.

In this work, the Pennes bioheat equation was be used to simulate bioheat transfer in the human body, and the model that represents heat exchange on the circulatory system described in Fiala (1998) was implemented in a three-dimensional finite element code to simulate hypothermia treatments in adults. The in-house software was developed at the Structure and Materials Laboratory at the Federal University of Rio de Janeiro. It is a continuation of the work of Silva (2012, 2016). Numerical analyses of whole body cooling methods were performed to compare the efficacy of of cooling mattress and intravascular catheter procedures during rapid cooling, maintenance of cooling and rewarming phase of the therapy.

2 METHODOLOGY

2.1 Bioheat transfer

The transport of blood in a living tissue is a difficult process to be modeled at the microscopic level due to the large amount of vessels present in the tissues and the internal processes that participate in heat transfer and change with temperature. The appropriate handling of the blood perfusion term and its thermal effect must be considered.

In this paper, the calculation of a whole body thermal analysis will be based on a continuum macro-scale bioheat model based on blood perfusion developed by Pennes (Bhowmik et al., 2013). The model was originally developed to simulate bioheat transfer in the forearm, but extensions of this model to whole-organism calculations have been performed previously in literature with good results (Fiala, 1998; Laszczyk and Nowak, 2015a; Vallez et al., 2016; Zhu et al., 2009).

This bioheat model considers blood and tissue as a continuous homogeneous medium. The Pennes' equation is given by

$$\rho_t c_t \frac{\partial T_t}{\partial t} = \nabla \cdot (k_t \nabla T_t) + \rho_b c_b \omega_b (T_a - T_t) + \dot{q}_m \tag{1}$$

and represents the bioheat flux in a domain Ω . In the above equation, the left-hand side accounts for the unsteady term, the first term on the right represents the conductive heat transfer through the tissue, the second entry on the right-hand side is the blood perfusion heat convection term and the last term is the energy generation associated with metabolism. The symbol T is the temperature and the subscripts t, b, a and m represent tissue, blood, arterial blood and metabolism, respectively. The material properties defined in the equation are: k (thermal

conductivity), c (specific heat), ρ (density) and ω (blood perfusion rate). The metabolic heat generation rate is represented by $\dot{q}_m$. The values of the parameters will be defined in the next chapter. The perfusion term and the metabolic heat generation rate are considered as isotropic heat sources. The arterial temperature T_a is obtained considering the heat exchanges during blood circulation in the body, and will be discussed in the next section.

The bioheat equation is defined in all parts of the body considering different properties for each tissue. The boundary conditions are prescribed temperatures $\overline{T}(\Gamma_t.t)$ in the boundary Γ_t and heat fluxes $\overline{q}(\Gamma_q, t)$ in the boundary Γ_q, $\Gamma = \Gamma_t \cup \Gamma_q$. The initial condition is,

$$T(x, t_0) = T_0, \tag{2}$$

where T_0 is the initial temperature in the tissue.

2.2 Metabolism

The metabolic heat generation rate in a specific tissue can be considered as a composition of the basal rate $\dot{q}_{m,0}$, representing a thermal neutrality condition, and an additional rate $\Delta\dot{q}_m$ generated by a local thermoregulation activity (Fiala, 1998):

$$\dot{q}_m = \dot{q}_{m,0} + \Delta\dot{q}_m \tag{3}$$

The additional rate $\Delta\dot{q}_m$ can be divided into three components:

$$\Delta\dot{q}_m = \Delta\dot{q}_{m,0} + \Delta\dot{q}_{m,sh} + \Delta\dot{q}_{m,w} \tag{4}$$

where $\Delta\dot{q}_{m,0}$ refers to local basal metabolic variation and $\Delta\dot{q}_{m,sh}$, $\Delta\dot{q}_{m,w}$ are variations due to changes in metabolism caused by shivering and muscular effort, present only in muscular tissues. The local basal metabolic variation occurs in muscular and non-muscular tissues, and reflects the dependence of the biochemical reactions on the local temperature of the tissue. It is a result of the van't Hoff Q_{10} effect (Fiala et al., 1999), and can be calculated by the equation:

$$\Delta\dot{q}_{m,0} = \dot{q}_{m,0}[Q_{10}^{\frac{T_t - T_0}{10}} - 1] \tag{5}$$

In the above equation, the reference temperature T_0 is the equilibrium temperature of the body equal to 30.0^oC and the Q_{10} coefficient is responsible for changes on the metabolic heat generation rate and blood perfusion rate due to changes in the temperature of the tissues, usually considered as equal to 2 (Fiala et al., 2012). The second and third terms in Eq. 4, $\Delta\dot{q}_{m,sh}$ and $\Delta\dot{q}_{m,w}$, were not considered in the cases simulated in this thesis, because of the particularities of the applications. The shivering effect may be neglected because it may be controlled in a medical procedure for adults. The muscular response may also be omitted since it is not the object of this study and the hypothermia treatment does not involve muscular activities that may increase the metabolic heat generation at a significant level.

2.3 Blood Circulatory System

The perfusion term in Eq. (1) considers that the heat exchange between blood and tissues occurs only on the capillary vessels, neglecting the heat exchange between adjacent arteries and veins in the body extremities, where the blood is colder than in the core. To consider

these effects and the changes in the arterial blood temperature (input of the Pennes equation) influenced by tissues temperature, the arterial temperature calculation is obtained using the circulatory system model described by Fiala (1998), assuming a non-uniform distribution of arterial temperature in the human body.

The main hypothesis of this circulatory model is that a central blood pool supplies the tissues through the main arteries. A counter current heat exchange between adjacent arteries and veins occurs before the blood reaches the capillary vessels. In this heat exchange, the arteries lose heat and the veins are rewarmed while flowing back to the central blood pool. The venous blood from the whole body is gathered in the blood pool and a new arterial temperature is obtained.

The model assumes the body is divided into different sectors. The central sectors have an arterial temperature equal to the blood pool temperature while the arterial temperature of the extremities is influenced by the countercurrent heat exchange effect. Assuming mass continuity in blood vessels and the net flow rate from the equation of gordon (Gordon, 2001), the arterial temperature can be calculated as:

$$T_a = \frac{\dot{m}_b \, c_b T_p + h_x T_v}{\dot{m}_b \, c_b + h_x} \tag{6}$$

The symbol T_p stands for the blood pool temperature, T_a and T_v are the arterial and venous temperature and h_x is the counter current heat exchange coefficient, considered as zero in the core and with defined values for the extremities of the body (Fiala et al., 1999).

The venous temperature T_v is assumed to be in equilibrium with the surrounding tissue, and the calculation of T_v in a body element can be obtained as follows:

$$T_{v_{element}} = \frac{\int \omega_b \, T_t \, dV}{\int \omega_b \, dV} \tag{7}$$

This means the venous blood leaving the body element is equal to the local tissue temperature of the element.

As described in Fiala et al. (2012), the blood pool temperature T_p is assumed to be a function of the tissue temperature in the whole body. However, in that implementation the body was divided into sectors with mutiple axisymmetric layers of tissues and the heat transfer equations between skin and external environment are coupled with the heat equation within tissue zones and between tissues, representing a compartimental model.

The implementation presented here is similar to the model applied for neonates described in Laszczyk and Nowak (2015a); Silva et al. (2016), and is a fully continuum three-dimensional model that considers that all sectors of the body are connected and heat is exchanged across all surfaces of each segment. The numerical procedure to calculate T_a, T_v and T_p will be shown in Section 2.7.

2.4 Blood Perfusion Rate

The blood perfusion rate $\omega_{b,t}$ in a specific tissue can be divided into two components:

$$\omega_{b,t} = \omega_{b,0,t} + \Delta\omega_{b,t} \tag{8}$$

where $\omega_{b,0,t}$ is the local basal blood perfusion rate and $\Delta\omega_{b,t}$ is a local variation depending on the tissue temperature, calculated as:

$$\Delta\omega_{b,t} = \omega_{b,0,t}\Big[Q_{10}^{\frac{T_t - T_0}{10}} - 1\Big] \tag{9}$$

Similarly to 5, the reference temperature T_0 is the equilibrium temperature of the body and the Q_{10} coefficient is usually considered as equal to 2.

2.5 External Heat Exchange

The heat exchange between the body and the surrounding environment can be divided into three main mechanisms: convection, radiation and evaporation. The heat exchange rate varies along the body surface, and the heat flux is the sum of the contributions of convective, radiative and evaporative fluxes:

$$q_{skin} = q_{conv} + q_{rad} + +q_{evap} \tag{10}$$

The convective flux q_{conv} between the skin surface and the external environment can be calculated using the Newton cooling law, defined as

$$q_{conv} = h_{conv} \,.\, (T_{ext} - T_{skin}) \tag{11}$$

The symbols T_{ext} and h_{conv} indicate the external temperature and the heat transfer coefficient, respectively.

The radiative flux between the skin and the surrounding environment can be obtained by the Stefan-Boltzmann law:

$$q_{rad} = h_{rad}(T_{skin}^4 - T_{sr,mean}^4) \tag{12}$$

where T_{skin} is the temperature at the skin surface, $T_{sr,mean}$ is the mean temperature of the surrounding radiating surfaces and

$$h_{rad} = \sigma\, \varepsilon \tag{13}$$

in which σ refers to the Stefan-Boltzmann constant and ε is the average emissivity of all radiating surfaces. The emissivity may vary depending on the surface material (skin, clothes, hair).

The evaporative flux was incorporated in the model as a prescribed heat flux boundary condition to consider heat losses by evaporation, based on values described in the literature.

Respiration losses were incorporated on the material thermal properties of the trunk/head sectors, as respiration can be responsible for a loss of 25% of whole-body metabolic heating Vallez et al. (2016).

2.6 Lumped Analysis for Blood Cooling

One of the most effective ways to reduce body temperature is to use intravascular cooling catheters, that directly cools the major veins and can achieve cooling rates of $5.0^oC/hour$ depending on the capacity of the device Dae et al. (2003). In these procedures, the blood temperature is actively lowered or increased. The simulation of blood cooling for hypothermia

treatments using methods applied directly to the blood vessels, as intravenous saline fluid infusion or an intravascular catheter, needs an additional method coupled to the Pennes bioheat equation to account for the tissue-blood thermal interactions.

In this paper, we implemented a model that considers the energy balance of a blood compartment as a lumped system that combines the energy added or subtracted by a external device and the loss of heat from blood to tissues during circulation. This model, adapted from Zhu et al. (2009), provides a method to obtain blood and body temperatures during active blood temperature modifications and is capable of simulating the stages of cooling and rewarming of blood during hypothermia procedures to treat strokes and brain damages in adults.

The mathematical formulation couples the Pennes bioheat equation (Eq. 1) and an equation of energy balance of the blood compartment of the body. The energy balance can be described as

$$\rho_b c_b V_b \frac{dT_a}{dt} = Q_{ext}(T_a, t) - Q_{b-t}(t) = Q_{ext}(T_a, t) - \rho_b c_b \overline{\omega} V_{body}(T_a - \overline{T_t}) \tag{14}$$

where Q_{ext} represents the capacity of the external device and can be a function of arterial temperature or time, and V_{body} stands for the volume of the body. The parameter $\overline{\omega}$ is the mean volumetric blood perfusion rate, calculated by:

$$\overline{\omega} = \frac{1}{V_{body}} \int_{V_{body}} \omega dV_{body} \tag{15}$$

and $\overline{T_t}$ is the weight-average tissue temperature, defined by the relation:

$$\rho c \omega (T_{a0} - \overline{T_t}) V_{body} = \int_{V_{body}} \rho c \omega (T_{a0} - T_{t0}) dV_{body} \tag{16}$$

where T_{a0} stands for the arterial temperature before time step $t + \Delta t$ and T_{t0} represents the tissue temperature before time step $t + \Delta t$. At steady-state, the arterial temperature T_a should be the same as the weight-average tissue temperature $\overline{T_t}$.

The numerical procedure for the implementation of this model will be shown in the next section.

2.7 Numerical Model

In the numerical model, the finite element method is used to obtain an approximate solution to the Pennes equation and the circulatory model described in section 2.4. To solve the transient problem, a time-marching scheme based on a semi-discrete form of the FEM is used, where the spatial discretization is performed by finite elements and the time derivative is approximated by finite difference operators using the two-point closed Newton-Cotes formula, also called Trapezoidal rule. Considering the Pennes Eq. (1) in a spatial domain Ω and a temporal interval $(0, \Pi)$, the domain Ω is discretized into elements and at each time step $t = t_{n+1}$, the following system of algebraic equations is obtained:

$$M\,\dot{T}_{n+1} + K\,T_{n+1} = F_{n+1} \tag{17}$$

where M is the mass matrix, $\dot{T}_{n+1}$ are the nodal values of the time derivative of temperature, K is the stiffness matrix, T_{n+1} are the nodal temperatures at time step t_{n+1} and F_{n+1} is the vector of independent terms.

For the blood circulatory system, the counter current heat exchange and the circulatory system effects on blood pool temperature are incorporated by calculating the arterial temperature in each sector $T_{a,k}$ as

$$T_{a,k} = \frac{\rho_b \, c_b\Big(\sum_{i=1}^{N_k} \omega_{b,t,k} \, V_{i,t,k}\Big) \; T_p + h_{x,k} T_{v,k}}{\rho_b \, c_b\Big(\sum_{i=1}^{N_k} \omega_{b,t,k} \, V_{i,t,k}\Big) + h_{x,k}} \tag{18}$$

where the subscript k denotes the sector of the body, N_k is the number of elements in each sector k and $V_{i,t,k}$ is the volume of element i of the tissue t in the sector k.

The blood pool temperature can be written as:

$$T_p = \frac{\displaystyle\sum_{k=1}^{K}\Big[\frac{\rho_b \, c_b\Big(\sum_{i=1}^{N_k} \omega_{b,t,k} \, V_{i,t,k}\Big) \; \rho_b \, c_b\Big(\sum_{i=1}^{N_k} \omega_{b,t,k} \, V_{i,t,k} \, T_{i,t,k}\Big)}{\rho_b \, c_b\Big(\sum_{i=1}^{N_k} \omega_{b,t,k} \, V_{i,t,k}\Big) + h_{x,k}}\Big]}{\displaystyle\sum_{k=1}^{K}\Big[\frac{\Big[\rho_b \, c_b\Big(\sum_{i=1}^{N_k} \omega_{b,t,k} \, V_{i,t,k}\Big)\Big]^2}{\rho_b \, c_b\Big(\sum_{i=1}^{N_k} \omega_{b,t,k} \, V_{i,t,k}\Big) + h_{x,k}}\Big]} \tag{19}$$

In the above equation, K is the total number of sectors in the body and $T_{i,t,k}$ represents the temperature of each element i of tissue t in sector k. In this way, at each new iteration of the system, before assembling the stiffness matrix and the force vector, the temperatures $T_{a,k}$, T_p and $T_{v0,k}$ must be updated. A predictor multi-corrector algorithm is used for the treatment of the non-linearities Hughes (1987), as described in Silva et al. (2016).

For the method described in section 2.7 for blood cooling applications in adults, the transient problem represented by Eq. 14 can be discretized by finite differences. The implicit discretization scheme results in the calculation of arterial temperature as:

$$T_a^{n+1} = \frac{\frac{Q_{ext}\Delta t}{\rho_b c_b V_b} + T_a^n + \overline{T_t^n}\,(\frac{\rho_b c_b \overline{\omega} V_{body} \Delta t}{\rho_b c_b V_b})}{1 + \frac{\rho_b c_b \overline{\omega} V_{body} \Delta t}{\rho_b c_b V_b}} \tag{20}$$

In this case, the same iterative solver and element calculation procedure of the previous model is used. The calculation of the temperature T_a^{n+1} is performed before step 5 at each new time step.

3 APPLICATION

The geometrical model used for simulations in adults was obtained by segmentation of 3D medical images (CT scans) of the Visible Human Data Set (VHD) provided by the National Library of Medicine, Department of Health and Human Services (NLM). The medical images were used to generate a geometry using the software *MIMICS* and adapted using the softwares *ANSYS Workbench* and *Trelis* to generate a 13 million mesh of a male adult with a body weight of $100kg$, body surface area of $2.27m^2$, $1.88m$ height, a cardiac output of $6l/min$ and 28% body fat content. The total basal whole body metabolism is $106W$ and basal evaporation rate from the skin of $18W$ (taken from Fiala et al. (2012)).

The geometry consists of eight different materials (skin+fat, muscle, bone, brain, viscera, lungs, eyes and cerebrospinal fluid) divided in six sectors (trunk + abdomen, head, arm, hand, leg, foot). Only half of the body was used for the simulations, due to symmetry. The geometry of the adult, the materials and division into sectors can be seen in Figures 1-4.

The finite element mesh consisted of 13.0 million four-node tetrahedral elements. A zoom in the upper region of the body is shown in Figure 5.

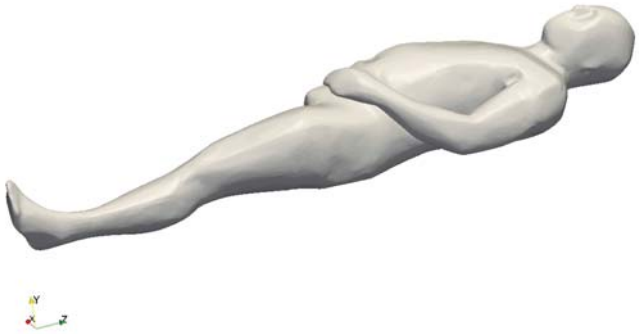

Figure 1: Geometry of the male adult

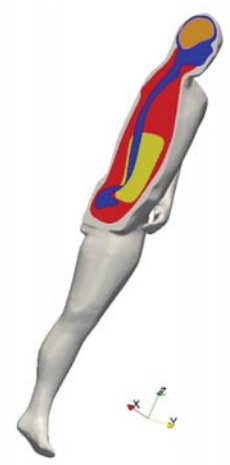

Figure 2: Geometry of the male adult, internal organs

The thermophysiological properties of the human tissues were taken from the literature, adapted from Vallez et al. (2016); Fiala (1998); Hasgall et al. (2015). Table 1 shows the material properties for each tissue used in this simulation. Metabolic heat generation rates used in the simulation considers the impact of respiration on heat loss corresponding to 25% of the whole-body metabolic heating Vallez et al. (2016), distributed over the elements belonging to the sectors trunk+abdomen and head. The counter current heat exchange coefficients were taken from Fiala (1998).

The first example used to validate the adult geometry and tissue properties in these simulations was taken from Vallez et al. (2016); Fiala et al. (1999) and consists of a male human subjected to a room environment in thermal neutrality (where no regulation occurs). The skin surface was exposed to a room temperature of 30.0^oC and a heat transfer coefficient value of $7.0W/m^2.^oC$ was used.

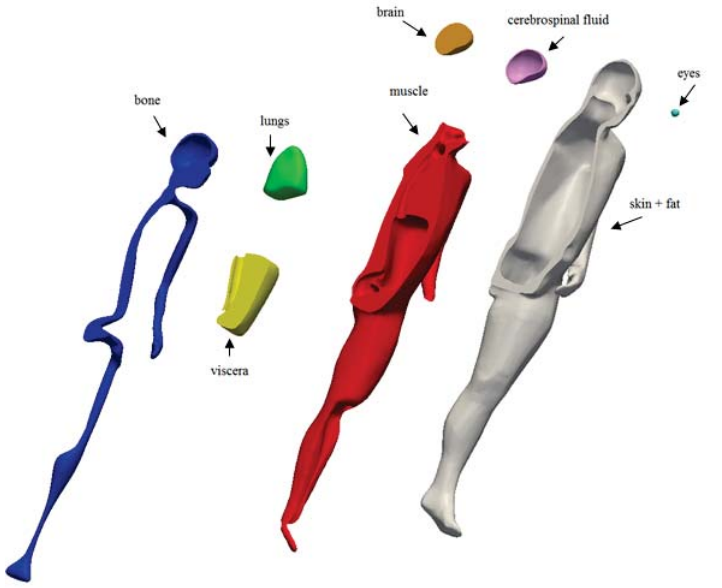

Figure 3: Geometry of the tissues - adult

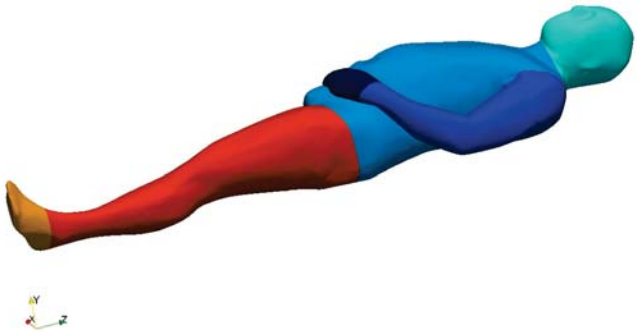

Figure 4: Division into sectors - adult

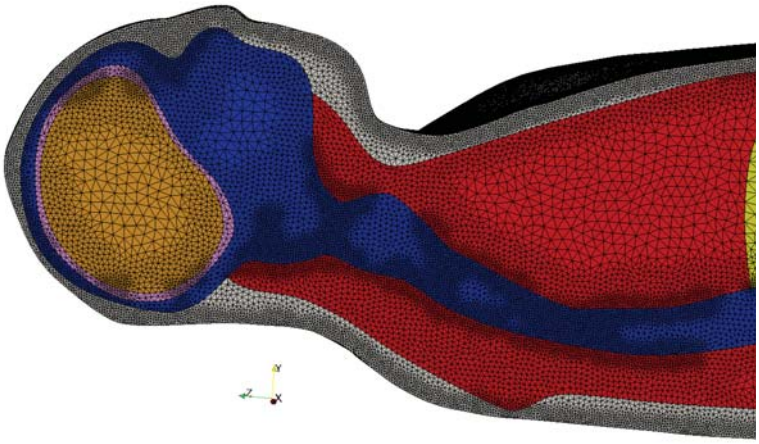

Figure 5: Zoom -Mesh of 13.0 **million elements**

Table 1: Thermophysiological properties of the different tissues - adults

Material properties					
Tissue	Thermal Conductivity ($W/m.^oC$)	Density (kg/m^3)	Specific Heat ($J/kg.^oC$)	Metabolic Heat Generation Rate (W/m^3)	Blood Perfusion Rate ($1/s$)
Blood	0.5	1050	3800	-	-
Eye	0.43	1076	4200	0	0
Lungs	0.39	394	3886	1835	0.0008677
Skin + Fat	0.2	877	2727	170	0.0003146
Cerebrospinal fluid	0.57	1007	380	0	0
Bones	1.16	1300	1590	0	0
Muscle	0.5	1050	3770	528	0.0005355
Viscera	0.55	1100	3350	3160	0.004532
Brain	0.53	1360	2450	12954	0.013124

The simulation of WBC procedure was based on temperature results found in different clinical studies Wang et al. (2004); Yang et al. (2006); Harris et al. (2009); Callaway et al. (2002) and the boundary conditions of numerical simulations Fiala (1998); Vallez et al. (2016); Laszczyk and Nowak (2015a) were considered to perform analyses that match the same values obtained in the clinical trials. The target was to reduce core temperature to around 34.0^oC after $1-4$ hours, maintaining the temperature at this level during 24 hours and then rewarming the body at a rate of $0.15-1.45^oC/hour$. Although the body temperature can be higher or lower than the normal temperature depending on the trauma, the examples presented in this work consider an initial body temperature of 37.0^oC.

Whole body cooling simulations were performed considering a cooling mattress on the bottom part of the body and a room environment for convective and evaporative heat fluxes on the top part. Both regions are depicted in Fig. 6.

For the top surface, a room temperature of 25.0^oC was prescribed and a convective heat transfer coefficient of $7.0W/m^2.^oC$ is used. The contact between body and cooling mattress is simulated by a convective flux prescribed at the bottom surface, considering an initial temperature of 10.0^oC during the first 2 hours of analysis. After this initial rapid cooling, the cooling mattress temperature is set to 33.0^oC during 22 hours. The convective heat transfer coefficient

Figure 6: Top (green) and bottom (black) surfaces used to prescribe boundary conditions in whole body cooling

was set to $10.0W/m^2.^oC$, based on experimental studies found in Vallez et al. (2016). A second subcase for performed considering a room temperature of 20.0^oC and comparing the results. After 2 hours of simulation the cooling mattress temperature has been set to 34.0^oC during the rest of the analysis.

For the case described for intravascular catheter cooling method, the same boundary conditions of the previous case is used. The mattress does not exchange heat and is considered as an insulated surface (no heat flux) during the first hour of simulation. After the first hour, the mattress temperature is set to 33.0^oC and the heat transfer coefficient of $10.0W/m^2.^oC$ is used. The top surface is subject to a convective flux with a heat transfer coefficient of $7.0W/m^2.^oC$. The heat exchanged by the device is $100W$ during the first hour of simulation; after this period, the device is turned off. The idea is to use the device for rapid cooling and then maintain the temperature at a hypothermia level using a cooling mattress.

4 RESULTS

In the first case, conditions of thermal neutrality were imposed and a transient simulation was performed until a steady-state solution was obtained. The core temperature was extracted and compared to normothermic values of a human subject to a 30.0^oC room temperature. The results showed a core temperature of 37.0^oC, in agreement with values from other studies Vallez et al. (2016); Fiala (1998). The mean skin surface temperature was 34.3^oC, consistent with the results of published data for neutrality conditions described by Fiala (1998), where the mean skin surface temperature of 34.4^oC has been obtained.

The second case analyses core temperature during a whole body cooling treatment using a cooling mattress. Figure 7 shows changes in blood pool temperature during the 24 hour procedure.

The results show a drop in the blood pool temperature to 34.0^oC after 2 hours of simulation and the core temperature reaches the minimum value of 33.8^oC at the end of the simulation. A temperature profile at the end of the analysis at the outer skin and internal organs is depicted in Fig. 8 and Fig. 9.

The temperature profile shows a minimum brain temperature of 34.1^oC at the end of the simulation. The temperature distribution at the top skin surface has a range of temperature between $24.6 - 30^oC$, and the minimum values are found in the extremities (hands and feet).

The third case considers the anatomical geometry for simulation of direct blood cooling treatment. The simulation of an invasive procedure using an intravascular catheter for an adult uses an insulated mattress during the first hour of simulation and a room temperature of 25.0^oC.

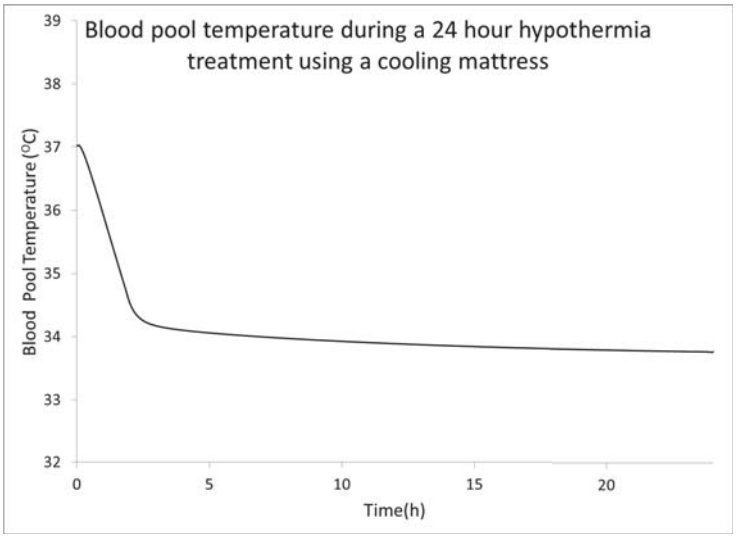

Figure 7: Second case - Adults: Core temperature during a 24 hour treatment using a cooling mattress.

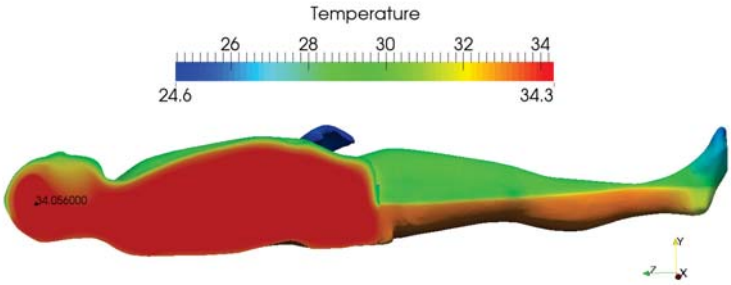

Figure 8: Second case - Adults: internal temperature distribution after a 24 hour treatment.

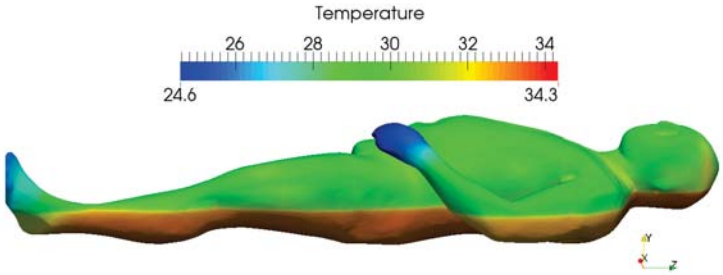

Figure 9: Second case - Adults: skin temperature distribution after a 24 hour treatment.

The blood cooling procedure is treated as an external device with capacity of $100.0W$ applied during the first hour of simulation. After the first hour, the mattress temperature is set to 33.0^oC with a heat transfer coefficient of $10.0W/m^2.^oC$ and the intravascular catheter is turned off. Results of arterial temperature during 24 hours are shown in Fig. 10.

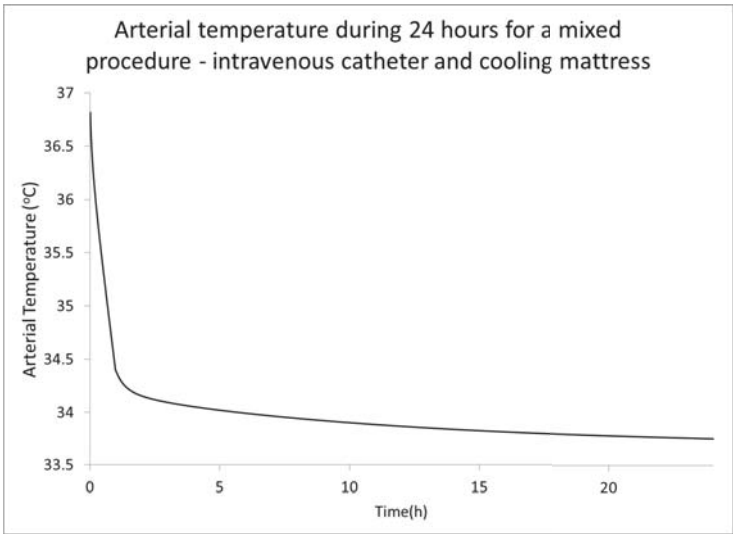

Figure 10: Third case - Adults: Arterial Temperature during 24 hours of a mixed hypothermia procedure - intravenous catheter and cooling mattress.

The results show a drop in arterial temperature of 2.6^oC during the first hour of simulation. After this period, the cooling rate is reduced and the temperature drops from 34.4^oC to 33.6^oC during the next 23 hours of simulation.

5 CONCLUSION

The main goal of the work described in this paper was to develop a finite element model able to simulate bioheat transfer processes in adults, and to perform whole body cooling procedures as a treatment for brain traumas in adults. The Pennes bioheat model was chosen to simulate the bioheat transfer processes in a macroscale and the blood pool approach described in Fiala (1998) was considered to take into account changes in the arterial temperature due to the circulatory system and heat transfer with the environment. For blood cooling using intravenous catheter, a blood cooling approach described in Zhu et al. (2009) was used.

The whole body cooling method applied to the adult body produced satisfactory results in reducing brain/core temperature to less than 34.0^oC in two hours. The moderate hypothermia was maintained for 22 hours with a core temperature around $34.0 - 33.8^oC$. As state previously, the brain temperature remained $0.2 - 0.3^oC$ above/below core temperature during the whole analysis.

The blood cooling simulation, considering an intravascular catheter, was able to reduce core temperature to less than 34.0^oC in one hour. After the intravascular catheter was removed, the cooling mattress was set to a temperature of 33.0^oC. The mixed method was able to simulate a hypothermia treatment with rapid cooling and maintanance of cooling at moderate hypothermia levels during 24 hours. Suggestion of a study using mixed methods, considering head cooling methods to maintain cooling after induction of hypothermia with cold intravenous fluids were mentioned in Harris et al. (2012), but no results were found in clinical trials mixing blood cooling with SBC or WBC methods.

The results of different cooling methods applied to adults demonstrate the importance of the model developed in this work for the study of different scenarios of cooling procedures. The

model presented here was capable to reproduce a hypothermic treatment in a realistic adult body with results similar to values reported in the literature Harris et al. (2012); Hoque et al. (2010); Unit (2006). This opens the way for the optimization of the treatment on a patient-specific basis.

Calibration of the model using real hypothermia cases could be used as a start to test cost-effective methods for brain/body cooling. After validation, these tests could be used as a standard protocol in clinics and hospitals for public health care, reducing neurological damages after cerebral traumas. Also commercial hypothermia equipments could be improved, coupling an on-time simulation to the system that controls body temperature to predict what could be the most effective set up to reach the desired results.

Another issue concerns the lack of standardized practices used for hypothermia treatments. Although the benefits of hypothermia for post-traumic brain injuries in adults is widely known, the uncertainties about effectiveness and robust evidence of reducing brain temperature during clinical trials makes it difficult to define a cooling method to be used for each case of trauma. Whole body cooling is a promising method that still need further research and more robust proof of temperature reduction. Studies should describe clearly baseline temperatures, duration of cooling, temperatures achieved and temperature changes with cooling, along with side effects of each method. In this way, joint research between engineers and clinicians could fill some empty spaces in this issue and collaborate to reduce post-traumatic neurological damage in patients suffering brain traumas.

Although the development of this three-dimensional finite element model was conducted with the object to investigate hypothermia treatments, it can be also adapted to predict body temperature changes during exercises and different heat exposures. The numerical tool presented here can be improved and many additional time or temperature dependent parameters can be added to simulate transient body temperature in different applications.

Acknowledgements

We thank the Carlos Chagas Filho Research Foundation of the State of Rio de Janeiro (FAPERJ) and the Coordination for the Improvement of Higher Education Personnel (CAPES), both in Brazil, for the financial support.

REFERENCES

Al-Othmani, M., Ghaddar, N., and Ghali, K. A multi-segmented human bioheat model for transient and asymmetric radiative environments. *International Journal of Heat and Mass Transfer*, 51:5522–5533, 2008.

Bhowmik, A., Singh, R., Repaka, R., and Mishra, S. Conventional and newly developed bioheat transport models in vascularized tissues: A review. *Journal of Thermal Biology*, 38(3):107–125, 2013.

Callaway, C., Tadler, S., Katz, L., Lipinski, C., and Brader, E. Feasibility of external cranial cooling during out-of-hospital cardiac arrest. *Resuscitation*, 52:159–165, 2002.

Colbourne, F. and Corbett, D. Delayed and prolonged post-ischemic hypothermia is neuroprotective in the gerbil. *Brain Research*, 654:265–272, 1994.

Dae, M. W., Gao, D. W., Ursell, P. C., Stillson, C. A., and Sessler, D. I. Safety and efficacy of endovascular cooling and rewarming for induction and reversal of hypothermia in human-sized pigs. *Stroke*, 34:734–738, 2003.

Diao, C., Zhu, L., and Wang, H. Cooling and rewarming for brain ischemia or injury: Theoretical analysis. *Annals of Biomedical Engineering*, 31(3):346–353, 2003.

Eicher, D. J., Wagner, C. L., Katikaneni, L. P., Hulsey, T. C., Bass, W. T., Kaufman, D. A., Horgan, M. J., Languani, S., Bhatia, J. J., Givelichian, L. M., Sankaran, K., and Yager, J. Y. Moderate hypothermia in neonatal encephalopathy: efficacy outcomes. *Pediatric Neurology*, 32:11–17, 2005.

Fiala, D. *Dynamic simulation of human heat transfer and thermal comfort*. PhD thesis, De Montfort University, Leicester, UK, 1998.

Fiala, D., Lomas, K. J., and Stohrer, M. A computer model of human thermoregulation for a wide range of environmental conditions: the passive system. *Journal of Applied Physiology*, 87 (5):1957–1972, 1999.

Fiala, D., Havenith, G., Brde, P., and B. Kampmann, G. J. UTCI-fiala multi-node model of human heat transfer and temperature regulation. *International Journal of Biometeorology*, 56 (3):429–441, 2012.

Gordon, C. J. The therapeutic potential of regulated hypothermia. *Emergency Medicine Journal*, 18(2):81–89, 2001.

Harris, B., Andrews, P., Murray, G., Forbes, J., and Moseley, O. Systematic review of head cooling in adults after traumatic brain injury and stroke. *Health Technology Assessment*, 16 (45), 2012.

Harris, O., Muh, C., Surles, M., Pan, Y., Rozycki, G., and Macleod, J. Discrete cerebral hypothermia in the management of traumatic brain injury: a randomized controlled trial. *Journal of Neurosurgery*, 110(6):1256–1264, 2009.

Hasgall, P. A., Gennaro, F. D., Baumgartner, C., Neufeld, E., Gosselin, M. C., Payne, D., Klingenbock, A., and Kuster, N. IT'IS database for thermal and electromagnetic parameters of biological tissues. Virtual Population Group, 2015.

Hickey, R. W. and J.Painter, M. Brain injury from cardiac arrest in children. *Neurologic Clinics*, 24:147–158, 2006.

Hoque, N., Chakkarapani, E., Liu, X., and Thoresen, M. A comparison of cooling methods used in therapeutic hypothermia for perinatal asphyxia. *Pediatrics*, 126:e124–e130, 2010.

Hughes, T. J. *The Finite Element Method - Linear Static and Dynamic Finites Element Analysis*. Prentice-Hall International Editions, New Jersey, 1987.

Laszczyk, J. E. and Nowak, A. J. *The analysis of a newborn's brain cooling process - measurements and CFD modelling*. LAP LAMBERT Academic Publishing, Gliwice, 2015a.

Laszczyk, J. E. and Nowak, A. J. Computational modelling of neonates brain cooling. *International Journal of Numerical Methods for Heat and Fluid Flow*, 26(2):571–590, 2015b.

Nolan, J. P., Morley, P. T., Hoek, T. L. V., and Hickey, R. W. Therapeutic hypothermia after cardiac arrest. *An Advisory Statement by the Advanced Life Support Task Force of the International*

Liaison Committee on Resuscitation Writing Group, 108:118–121, 2003.

Nozari, A., Safar, P., Stezoski, S. W., Wu, X., Kostelnik, S., Radovsky, A., Tisherman, S., and Kochanek, P. M. Critical time window for intra-arrest cooling with cold saline flush in a dog model of cardiopulmonary resuscitation. *Journal of the American Heart Association*, 113: 2690–2696, 2006.

Silva, A. B. C. G. *Numerical analyses of the temperature distribution in the human brain using the finite element method*. MSc dissertation, Federal University of Rio de Janeiro, Rio de Janeiro, Brazil, 2012.

Silva, A. B. C. G. *A finite element thermoregulation model of the human body for hypothermia treatment in adults and neonates*. DSc thesis, Federal University of Rio de Janeiro, Rio de Janeiro, Brazil, 2016.

Silva, A. B. C. G., Laszczyk, J., Wrobel, L. C., Ribeiro, F. L. B., and Nowak, A. J. A thermoregulation model for hypothermic treatment of neonates. *Medical Engineering and Physics*, 38:988–998, 2016.

Tisherman, S. A. and Sterz, F. *Therapeutic Hypothermia*. Springer, San Francisco, 2005.

Unit, N. P. E. TOBY study protocol - whole body hypothermia for the treatment of perinatal asphyxial encephalopathy. volume 2. National Perinatal Epidemiology Unit, 2006.

Vallez, L. J., Plourde, B. D., and Abraham, J. P. A new computational thermal model of the whole human body: Applications to patient warming blankets. *Numerical Heat Transfer - Part A*, 69(3):227–241, 2016.

Wang, H., Olivero, W., Lanzino, G., Elkins, W., Rose, J., and Honings, D. Rapid and selective cerebral hypothermia achieved using a cooling helmet. *Journal of Neurosurgery*, 100:272–277, 2004.

Xiang, S. H. and Liu, J. Comprehensive evaluation on the heating capacities of four typical whole body hyperthermia strategies via compartmental model. *International Journal of Heat and Mass Transfer*, 51:5486–5496, 2008.

Yang, Y., Ou, X., and Chen, Q. A study on time of head hypothermy for large acreage cerebral infarction patients with central high fever. *Chinese Nursery*, 20:45–46, 2006.

Zhu, L., Schappeler, T., Cordero-Tumangday, C., and Rosengart, A. J. Thermal interactions between blood and tissue. *Advances in Numerical Heat Transfer*, 3:191–219, 2009.